ELSEVIER

Journal of Alloys and Compounds 279 (1998) 75–81

Journal of ALLOYS AND COMPOUNDS

Toward cellular automata: the role of atomistic simulation in determining material structures

Robin W. Grimes

Department of Materials, Imperial College, London SW7 2BP, UK

Abstract

The relationship between approximate atomistic computer simulation methods and experiment is examined in detail. Initial parameterisation of interionic potentials requires specific experimental data. However, simulations can then generate systematic relationships. Closer combination of atomic level experiment and simulation reveals a synergy with solutions to materials issues only being possible through a concerted use of both approaches. Finally the ability of atomistic level simulation to provide data for micro-scale problems is discussed.

Keywords: Molecular modelling; Atomistic computer simulation; Cellular automata; Ceramics

1. Introduction

Computer simulation techniques which develop models of matter at the atomic level have advanced rapidly in recent years. This has been driven partly by a growing awareness of the potential benefits of engineering materials at the nano scale. However, it has been enabled by the reduction in the cost of effective computing platforms, as greater power and memory have become available.

Two types of development have been possible. First, at the high end, increasingly accurate quantum mechanical methods have been pioneered, whose aim is to make reliable predictions independently of experiment [1,2]. Such computational demands mean that those methods can still only be applied to relatively simple systems and are generally limited to tens or, given large parallel machines, perhaps hundreds of atoms, depending on the task.

Unfortunately, many materials applications of atomic simulation require that we consider at the very least thousands of atoms. In addition, 'real' systems are usually multi-component (either by design or default) with the secondary phases, precipitates or impurities being critical factors in the control of performance. Thus, approximate methods continue to be important.

In ceramics, methods based on energy minimisation or molecular dynamics have been used to simulate a diverse complement of systems [3,4]. Such methods employ long range Coulombic forces and short range parameterised potentials. The computational simplicity of this description is commensurate with the task of modelling real materials in that it is possible to explicitly model the required number of ions. Of course, the approximations inherent in parameterised potential forms demand a particularly close connection with experiment both in verification of key results and in enabling the initial parameterisation to take place.

In what follows, the results of recent atomistic simulation studies of ionic ceramics will be considered in the context of their practical use to materials design, experimental interpretation and ultimately, fabrication control. Initially, certain aspects of methodology, as it relates to these issues, will be reviewed.

2. Methodology

2.1. Interionic interactions

Atomically pure ceramic materials are a myth. Ultimately, atomistic models must therefore be able to address the effect that either point, line or planar defects have on lattice structures. These defects disrupt the lattice and ions are displaced from their lattice sites. When a charged defect is introduced into a ceramic, the surrounding lattice will be in an electric field [5]. This causes ions to relax, that is, the surrounding material becomes polarised. To model this effectively the forces acting between hundreds of ions must be accounted for explicitly. In the examples discussed below, the interionic interaction energies between ions i and j, $E(r_{ij})$, are approximated using a

0925-8388/98/$19.00
PII: S0925-8388(98)00615-X

parameterised interionic potential form known as the Buckingham potential;

$$E(r_{ij}) = \frac{q_i q_j}{r_{ij}} + A_{ij} \exp(r_{ij}/\rho_{ij}) - \frac{C_{ij}}{r_{ij}^6} \quad (1)$$

where the first term is the long range Coulombic interaction and A_{ij}, ρ_{ij}, C_{ij} are adjustable parameters, specific to ions i and j.

Traditionally effective interatomic potential parameters have been derived by fitting to experimental data from the host lattice (e.g. lattice parameter, elastic constant and dielectric constant). It is becoming clear that this is not sufficient if the potential form is required to describe displacements of host ions away from their perfect lattice sites. This is particularly true for surfaces where displacements are often, though not necessarily, substantial (i.e. $>\sim$0.2 Å) [6].

Recently the approach to parameter derivation has been to start by calculating interaction energies as a function of separation, using an approximate quantum mechanical technique. The parameters of the potential function are then fitted to this potential energy surface. Subsequently the parameters are adjusted by fitting to the experimental data of not only the host lattice but of an appropriate number of additional structures. For example, when modelling planar defects in the SrO–$SrTiO_3$ system, the potential function which describes the interaction between Sr^{2+} and O^{2-} was fitted simultaneously to both the SrO and $SrTiO_3$ structures [7]. These parameters were then used to model the Ruddleston–Popper phases $Sr_{1+x}TiO_{3+x}$, which are formed from inter growths of SrO and $SrTiO_3$ the parameterisation is therefore clearly appropriate to the problem being addressed.

More recently, attempts to model the cement phase material Ca_2AlFeO_5 have been based on a fit of the Ca^{2+}–O^{2-} potential parameters simultaneously to $Ca_2Fe_2O_5$, $CaFe_2O_4$, $Ca_3Al_2O_6$, $CaAl_2O_4$ and CaO, in addition to Ca_2FeAlO_5. Again the phases used in the parameterisation reflect the type of coordinations and inter ionic separations to which the Ca^{2+} ion will be exposed in the defective material.

Finally, it is necessary to decide how to approach the problem of calculating the energy of an ion in a crystal which typically will be μm sized, i.e. will consist of $\sim 10^{11}$ ions. Fortunately, for ionic materials, the long range Coulombic force experienced by an ion in a period lattice can be determined using the Ewald summation technique [8,9]. The short range part of the potential (characterised by A_{ij}, ρ_{ij}, C_{ij}) is summed explicitly out to a few unit cell dimensions (~20 Å), beyond which it is negligible and therefore ignored.

2.2. Total energy calculations

Once the potentials describing the forces between ions are established the total energy of the system can be calculated. This will depend on the ion positions which must therefore be optimised in some manner. Three options are commonly used. The first is energy minimisation [10] which results in a quasi-harmonic average description of a static lattice. Data derived using this model can be compared to experiments with time scales that are long, with respect to atomic vibrations, (i.e. over a time greater than $\sim 10^{-11}$ s). Energy minimisation is typically achieved after approximately ten iterations.

Alternatively, by solving Newton's equations of motion, atomic vibrations can be modelled explicitly [11]. This molecular dynamic methodology (MD) leads directly to a prediction of kinetic effects and well defined thermodynamic parameters. The drawback to the method is that to derive data which can be usefully compared to experiment, many thousands of total energy calculations are necessary to achieve reasonable statistics.

The third optimisation technique is based on the Monte Carlo method [12,13] (MC) which yields information concerning atomic distributions at different temperatures. However, there is no explicit link to the kinetics of the system, although the system is allowed to evolve with time. In many ways, MC therefore occupies a position between energy minimisation and MD. In the examples discussed below only energy minimisation and MD methods were used.

Often the type of problem we will wish to consider is how to determine the change to the energy of the system due to the addition of defect ions. Two methods are typically employed. The first is based on periodic boundary conditions where a three dimensional cell of ions is repeated throughout space via a set of crystallographic vectors [14]. Of course, any change in ion population or position in a cell is also repeated throughout space in each cell [15] which means that each cell must be charge neutral.

The second approach is to define a large central region of ions whose positions and energies are treated explicitly. This is surrounded by an outer region in which ion positions are fixed. In this case, changes in defect population are made only in the central region and the effect on the outer region is approximated, typically as a dielectric response [4,5,10]. This approach can be used to model charged defects.

This short introduction into ceramic modelling has addressed some of the main features and focused on some of the critical issues in potential derivation. For more information, the reader is referred to recent compilations of papers and review articles [1–4,10,16–20]. The aim of this article is to focus on some practical results of the modelling work, so that the type of data that modelling studies can provide becomes clear.

3. Generation of relationships specific to a system

The importance of ion size on the thermodynamics and

kinetics of physical processes is well known. In ceramic materials it is clearly harder to accommodate a large ion at a lattice site formally occupied by a small ion. Nevertheless, if an ion can be accommodated at a site for which it is only a little too large, the resulting lattice strain may actually act to reduce the migration activation energy. The effect of ion size therefore has the potential to be quite subtle. As a consequence, studies of the systematic doping of specific systems may yield very useful predictive trends. Here, two examples will be considered: solution of divalent cations (i.e. MO) in a Y_2O_3 host lattice and isovalent substitution for Sr in the $Sr_3Ti_2O_7/SrTiO_3$ system [21].

3.1. Solution of MO in Y_2O_3

In the case of MO solution in Y_2O_3 (a refractory [22] and proton conductor [23]), the substitutional M^{2+} ions are charged so that solution is accompanied by charge compensating defects. Two low energy solution reactions present themselves:

$$3MO(s) \overset{Y_2O_3}{\rightarrow} 2M'_Y + M_i^{\cdot\cdot} + 3O_O^x \quad (2)$$

$$2MO(s) \overset{Y_2O_3}{\rightarrow} 2M'_Y + V_O^{\cdot\cdot} + 3O_O^x \quad (3)$$

The first mechanism proceeds via self-interstitial compensation and the second via oxygen vacancy compensation. If we assume that all the defect species remain far enough apart that there are effectively no inter-defect interactions, then the calculated solution energy, as a function of 2+ dopant ion radius [24] (see Fig. 1), shows a minimum at a radius corresponding to $\sim Cd^{2+}$ and the self-compensating mechanism is energetically the most favoured solution mechanism. On the other hand, if the inter-defect interactions are so strong that neutral defect clusters are formed (e.g. $\{Mg'_Y:Mg_i^{\cdot\cdot}:Mg'_Y\}^x$ or $\{Sr'_Y:V_O^{\cdot\cdot}:Sr'_Y\}^x$) for cations of higher radius, the oxygen vacancy mechanism is dominant (see Fig. 2), nevertheless

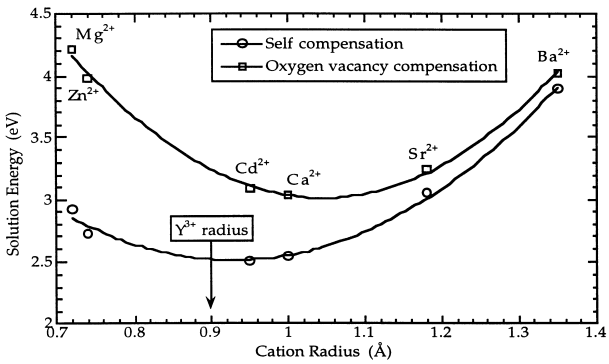

Fig. 1. Solution energies for the incorporation of MO into Y_2O_3 assuming isolated point defects.

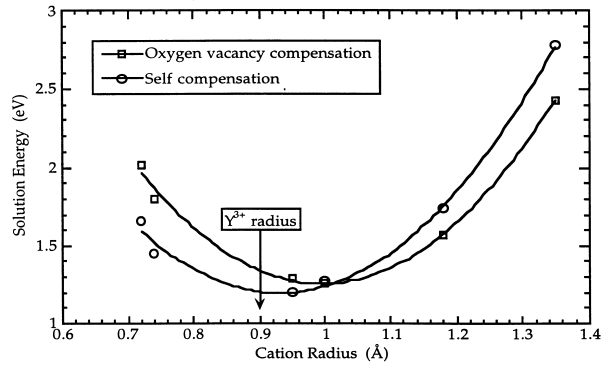

Fig. 2. Solution energies for the incorporation of MO into Y_2O_3 assuming the formation of neutral defect clusters.

the minimum in the solution energy remains around the Cd^{2+} radius.

The control of the oxygen vacancy population is important in controlling grain growth [22]. The systematics presented here show which size of substitutional ion will result in the greatest oxygen vacancy population and furthermore, which one will result in the most mobile oxygen vacancy (i.e. lowest binding energy given by the difference between the solution energies in Figs. 1 and 2). Neither are coincident with the lowest MO solution energy.

3.2. Segregation of M^{2+} dopant ions in the SrO–$SrTiO_3$ system

The second example concerns $SrTiO_3$, an important electronic ceramic used in capacitor and varistor devices, where control of the dielectric constant is critical. Again point defects can inhibit or enhance performance. Recent High Resolution Electron Microscopy (HREM) work [7] (discussed below) has shown that excess SrO in $SrTiO_3$ is accommodated in the form of a Ruddleston–Popper layer compound, $Sr_3Ti_2O_7$. Compositions between $Sr_3Ti_2O_7$ and $SrTiO_3$ form an intergrowth microstructure of these two materials. In such cases, a number of distinct Sr sites exist. One is associated with the parent $SrTiO_3$ perovskite phase. The Ruddleston–Popper phase $Sr_3Ti_2O_7$ provides two Sr sites. Lastly, at the (010) interface between $Sr_3Ti_2O_7$ and $SrTiO_3$ a forth site exists which is formed when a Sr^{2+} ion substitutes for a Ti^{4+} lattice site on the $Sr_3Ti_2O_7$ side of the interface. This substitution relieves lattice strain which results from Ti–Ti nearest cation neighbours (see Fig. 3).

The simulations predict that isovalent ions, substituting for Sr, become partitioned; large ions such as Ba^{2+} segregate to the (010) interface Ti substitution site while small ions such as Mg^{2+} remain in the parent perovskite phase. No ions prefer the sites in $Sr_3Ti_2O_7$. These results are presented schematically in Fig. 3.

In both the cases discussed in this section, the calculations predict the behaviour of point defects as a function of

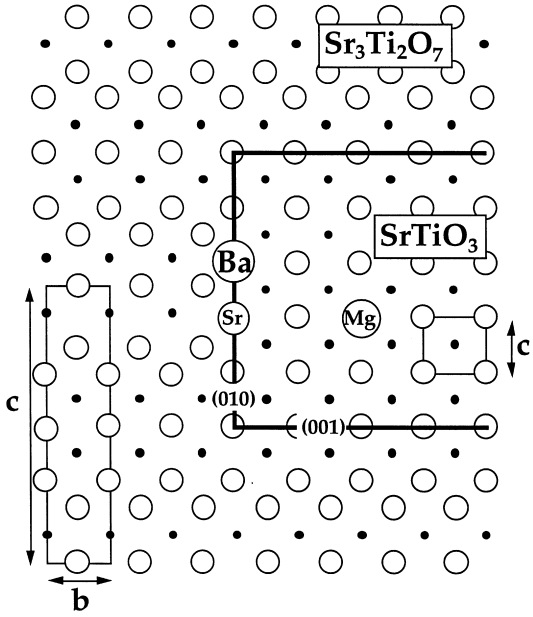

Fig. 3. Schematic diagram showing the [100] projection of the proposed cation sublattice of the $SrTiO_3/Sr_3Ti_2O_7$ intergrowth system. The solid circles are Ti^{4+} ions and the open circles Sr^{2+} ions, both on their usual lattice sites. In addition, the (101) interface shows two defects, a Ba^{2+} dopant ion and a Sr^{2+} ion substituted at a Ti^{4+} site. Finally a Mg^{2+} dopant ion is shown substituted at a Sr^{2+} lattice site in the $SrTiO_3$ parent phase.

a size parameter. In the first case, this information can be used to tailor an intrinsic-like defect population (i.e. the oxygen vacancy). In the second case the data indicates which size of dopant cation will segregate to a specific interfacial boundary. Certainly this type of approach could determine which size of cation will most effectively decorate a specific boundary. The aim of these studies is therefore to focus experimental work by providing an atomistic framework. Nevertheless, modelling and experiment are rather divorced from each other. In the next section, they are used in a more intimate manner.

4. Combining simulation and experiment

It is sometimes necessary to generate quite accurate atomistic data concerning structure and energetics. For complex systems, it is not always possible to be sufficiently confident about the data predicted through computer simulation alone. In such cases simulation can be combined with any appropriate experimental technique which is able to provide atomistic scale data. For example, recent HREM and simulation studies of $Zn_4In_2O_7$ were able to unambiguously determine that the space group of this transparent conducting oxide is $P6_3mmc$, consistent with a model proposed by Cannard and Tilley [25], rather than the alternative $P6_3/mmc$ model suggested by Kimizuka et al. [26] (see Fig. 4). It is important to note that it was impossible to unambiguously identify the

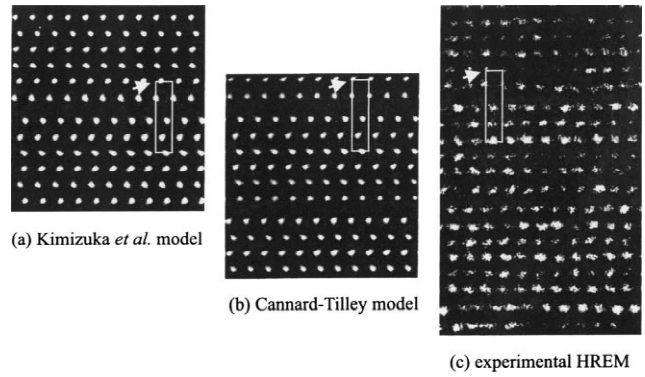

Fig. 4. Comparison of simulated HREM images of $Zn_4In_2O_7$ viewed in [1$\bar{2}$10] projection using (a) the Kimizuka et al. model and (b) the Cannard and Tilley model. These are noticeable differences in the two simulated images (arrowed) which correspond to differences in the structure of the indium-rich layers. The experimental micrograph is shown in (c).

structure solely on the basis of X-ray and electron diffraction results and only through the combined use of HREM and atomistic simulations could one clearly identify the structure of the material [27]. More specifically, the simulation provided detailed structural models for HREM image simulation which were verified by the experimental images.

The accuracy of the structural models lends credence to the analysis of energetics, in particular the relative stability of different In_2O_3–$(ZnO)_m$ phases. The *m*-even phases exhibited lower formation energies, relative to ZnO and In_2O_3, than did *m*-odd. During the experimental work it had been noted that *m*-odd phases were more difficult to form. The simulation results thus provided an atomistic explanation of the experimental observation.

The close correspondence between HREM and simulation, and the explanation of the relative stability of *m*-even, *m*-odd stability provides the confidence necessary for subsequent predictions – in this case, the formation energies of Zn^{3+} point defects in ZnO [27]. As with all the other examples discussed, appropriate parameterisation was the key. In this case, the Zn^{2+}–O^{2-} potential parameters were fitted to three polymorphs of ZnO and a similar procedure was employed for the In^{3+}–O^{2-} potentials.

The combination of HREM and simulation was also used to model the $Sr_3Ti_2O_7/SrTiO_3$ intergrowth microstructure described in Section 3.2 [7]. Synergy between the experiment and simulation was even more evident in this case. For example, the energetics of SrO solution in $SrTiO_3$ predicted the $Sr_3Ti_2O_7$ phase to be sufficiently more stable than other Ruddleston–Popper phases (e.g. $Sr_4Ti_3O_{10}$) for the intergrowth microstructure to form (see Fig. 5) rather than a single average structure, the key reaction enthalpy being:

$$Sr_4Ti_3O_{10} \Rightarrow Sr_3Ti_2O_7 + SrTiO_3 \quad \Delta E = -0.02\ \text{eV} \qquad (4)$$

In addition, it was possible to describe the atomic structure of the defect stabilised (010) interface between $Sr_3Ti_2O_7$

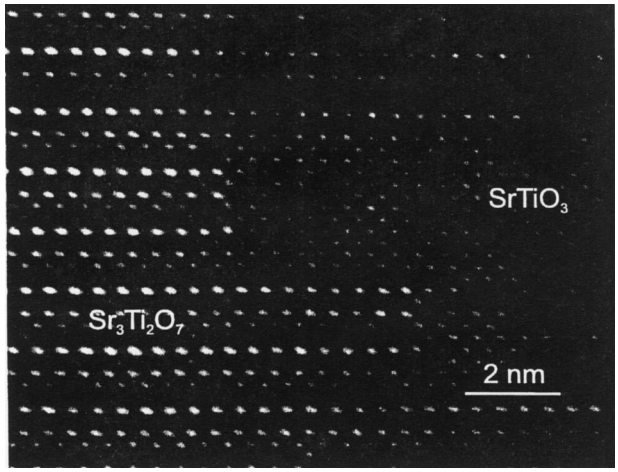

Fig. 5. HREM image showing intergrowth consisting of $SrTiO_3$ perovskite surrounded by $Sr_3Ti_2O_7$ Ruddleston–Popper; both phases are oriented in [100] projection.

and $SrTiO_3$. The number of possible combinations of defects makes conventional image simulation impractical. Atomic simulation can be used to rule out all but a few likely candidates (in this case, the specific Sr substitutions at Ti sites).

5. Calculations of dynamic effects

The efficacy of simulation can be measured in either its ability to reduce experimental effort or provide reliable information that is otherwise beyond present experimental capabilities. Although the examples discussed so far clearly fulfil these criteria (to differing extents) they have all been rather labour intensive; the ion positions and structures have to be chosen specifically. This is mainly because these examples have used energy minimisation to predict ion positions (see Section 2.2). This method relies on the user providing ion coordinates close to, although by no means exactly, near to their equilibrium positions. This can be an advantage in that it is possible to acquire data concerning local minima, i.e. meta-stable structures.

The other two ways of optimising ion coordinates, molecular dynamics (MD) and Monte Carlo (MC), to a significant extent use the computer to optimise ion positions. Consequently they are more computationally intensive and one should be aware that it is still possible for structures to be trapped in local energy minima. Nevertheless, the data that MD in particular can provide is beyond the scope of energy minimisation methods.

Recent simulations of nanocluster dynamics of LaF_3 have shown how the details of migration mechanisms can be uncovered [28] (refer to http://www.tms.org/pubs/joumals/JOM/9704/Bulatov/). For example, although the fluorine sublattice becomes disordered at 1100 K, ion migration is facilitated by a hopping mechanism or mechanisms which are mediated by at least one interstitial and one lattice site. Also, migration of F^- ions on the surface is slower than in the bulk. These results will have important consequences for the interpretation of fast ion diffusion in materials with a high density of grain boundaries.

One problem of using MD and to some extent MC, is that the description of forces must be very reliable since the potential energy surface being probed can be quite extensive. Although this presently limits the application of MD, it may be possible to update simple force descriptions using quantum mechanical techniques. Indeed, quantum mechanical procedures are already being used in conjunction with MC and MD algorithms, although the computational restrictions are dramatic.

Results of MD simulations are often hard to convey in a static format. Thus, electronic publications offer an excellent medium for understanding the dynamic effects. As such to view the results of this model, the reader is referred to a recent electronic paper which provides the necessary interactive interface [28].

6. Extending beyond small scale modelling

The small length scale and, for MD, small time scale inevitably restricts the use of atomistic simulation. To overcome this, it is necessary to use atomistic simulation to provide parameters for more general relationships. Simple examples of this are the ion size effects discussed in the first section although these maintain the small length scale. To make contact with large scale phenomena it is necessary to provide data for macroscopic relationships. Recent work shows that this should be possible. For example, the behaviour of quite small clusters of LaF_3 (up to 3120 atoms) already exhibit features that may be described by simple classical analysis [29]. In particular, it has been shown that the overall oscillations in the shape of the solid nanoclusters agree very well in frequency and magnitude with those deduced from classical elasticity theory. Furthermore, in the liquid phase, the droplet oscillations which are seen in the MD simulations have frequencies which show that the surface tension of the simulated droplet is typical of experimentally determined surface tensions for ionic systems. It would be a small step to carry out systematic investigations of the effect that impurities have on surface tension, something which is notoriously difficult experimentally.

Nevertheless, many problems remain. For example, during the macroscopic evolution of a system (e.g. in melting, grain growth or thin layer deposition) what is happening on an atomistic level may be quite different from one place to another, due to thermodynamic or compositional inhomogeneities. Furthermore, geometric changes are likely to move through (or across) the material in a non-uniform manner. Clearly atomistic modelling can

predict data pertinent to a local evolution but there is a limit to the number of ions that can be modelled, even with approximate methods. One way of overcoming this problem is to model the system as a set of discrete regions each subject to the effect of its environment, i.e. to specific but continuously or discretely changing (i.e. updated) boundary conditions. Again, the problem can become excessively convoluted since there are likely to be a very large number of complex states.

An attractive and computationally tenable solution is to carry out a limited series of atomistic simulations, of a representative set of discrete regions, subject to a variety of local boundary conditions. This provides a database which can be accessed by a macroscopic modelling technique. If the system evolves beyond the database, it is updated by the atomistic simulation method. Since the boundary condition is local, it could be translated into a local rule so that cellular automata would be an ideal macroscopic modelling technique.

Recently, Zacate et al. [30] (refer to http://abulafia.mt.ic.ac.uk/USAF/) have made some progress using cellular automata for molecular modelling by considering the evolution of inert gas islands on a metal surface. In this case, the number of possible states that each gas atom could attain was limited since the interactions were strictly nearest neighbour. Consequently, all the atomistic scale energetics associated with gas atom attachment and evaporation could be determined before any microstructural evolution took place. A series of constant temperature simulations were then carried out. The results predicted that the rate at which gas atom islands grow (or coarsen) was a strong function of temperature. At low temperatures this rate was slow but the rate increased steadily with temperature. However, beyond a certain temperature evaporation now occurred so quickly that the growth rate fell rapidly even though the total surface coverage was still considerable.

Future work is planned, and of particular interest is the pursuit of cellular automata in conjunction with alternative molecular modelling methods to significantly improve computational tractability.

7. Summary

Atomistic simulation methods have a variety of roles to play in the design of new materials. The examples in Section 3 show how approximate rules can be generated which can act as quantitative guides to the formation of specific structures. This does not require a particularly close relationship between simulation and experiment. On the other hand, intimate connections can pay dividends as demonstrated in Section 4. Indeed, there is a clear synergy when HREM and simulation are used. Together, through this duel development, it is possible to use simulation to provide an atomistic framework for the explanation of experimental results. However, to develop their full potential, atomistic simulation calculations must be linked with macroscopic modelling techniques. This will result in an understanding of how specific changes on the atomistic level alter or control the microstructural evolution of ceramic materials.

Acknowledgements

The computing facilities for this project were provided by the EPSRC through grant GR/K74302. I would like to thank Drs. M.A. McCoy and W.E. Lee who were instrumental in all of the HREM work. G. Busker and M.O. Zacate are thanked for various calculations but more particularly for their general support.

References

[1] E. Wimmer, Computational materials design with first-principles quantum mechanics, Science 269 (1995) 1397.
[2] F. Wimmer, Computational materials design and processing-perspectives for atomistic approaches, Mat. Sci. Eng. B-Solid State Mat. Adv. Technol. 37 (1996) 72.
[3] R.W. Grimes, A.H. Harker, A.B. Lidiard (Eds.), Interatomic Potentials, Philos. Mag. B, 73 (1) (1996).
[4] C.R.A. Catlow, A.M. Stoneham (Eds.), Computer simulation of defects in polar solids, J. Chem. Soc. Faraday Trans. 2; 85(5) (1989).
[5] N.F. Mott, M.J. Littleton, Conduction in polar crystals. I. Electrolytic conduction in solid salts, Trans. Faraday Soc. 34 (1938) 485.
[6] S. Vyas, R.W. Grimes, D.H. Gay, A.L. Rohl, The structure, stability and morphology of stoichiometric ceria crystallites, J. Chem. Soc. Faraday Trans. 94 (1998) 427.
[7] M.C. McCoy, R.W. Grimes, W.E. Lee, Phase stability and interfacial structures in the SrO–$SrTiO_3$ system, Philos. Mag. A 75 (1997) 833.
[8] P.P. Ewald, Ann. Phys. 64 (1921) 253.
[9] C.R.A. Catlow, M.J. Norget, Lattice structure and stability of ionic materials, UKAFA Harwell Lab., Report AERE-M2936, 1976.
[10] C.R.A. Catlow, W.C. Mackrodt, Theory of simulation methods for lattice and defect energy calculations in crystals, in: Computer Simulation of Solids, chapter 1, vol 166, Springer-Verlag, Berlin, 1982.
[11] M.P. Allen, D.J. Tildesley, Computer Simulation of Liquids, Oxford: Clarendon, 1987.
[12] S. Ling, M.P. Anderson, Monte-Carlo simulation of grain growth and recrystallization in polycrystailine materials, J. Min. Metals Mater. Soc. 44 (1992) 30.
[13] K. Binder, Atomistic modelling of materials properties by montecarlosimulation, Adv. Mat. 4 (1992) 540.
[14] R.A. Jackson, J.E. Huntingdon, R.G.J. Ball, Defect calculations beyond the dilute limit, J. Mat. Chem. 1 (1991) 1079.
[15] S. Vyas, R.W. Grimes, J.D. Binks, F. Rey, Metastable solid solutions of alumina in magnesia, J. Phys. Chem. Solids 58 (1997) 1619.
[16] C.R.A. Catlow, G.D. Price, Computer modelling of solid-state inorganic materials, Nature 347 (1990) 243.
[17] J.H. Harding, Computer simulation of defects in ionic solids, Rep. Prog. Phys. 53 (1990) 1403.
[18] A.H. Harker, R.W. Grimes (Eds.), The practical calculation of interionic potentials in solids; Mol. Simul. 4(5), 5(2) (1989).
[19] C.R.A. Catlow, A.M. Stoneham, J.M. Thomas (Eds.), New methods

for modelling processes within solids and at their surfaces, Philos. Trans. R. Soc. London, Ser. A 341 (1992).
[20] J.H. Simmons, E.R. Fuller Jr., A.L. Dragoo, E.J. Carbocyi (Eds.), Computational modelling of materials and processing, Adv. Ceram. 69 (1997).
[21] R.W. Grimes, G. Busker, M.A. McCoy, A. Chroneos, J.A. Kilner, S. Chen, The effect of ion size on solution mechanism and defect cluster geometry, Ber. Bunsenges. Phys. Chem. 101 (1997) 1204.
[22] P. Chen, I. Chen, Grain boundary mobility in Y_2O_3: defect mechanism and dopant effects, J. Am. Ceram. Soc. 79 (1996) 1801.
[23] Y. Larring, T. Norby, P. Kofstad, Protonic conductivity in Ca-doped yttria, Solid State Ionics 49 (1991) 73.
[24] R.D. Shannon, Revised effective ionic radii and systematic studies of interatomic distances in halides and chalcogenides, Acta Crystallogr. A32 (1976) 751.
[25] P.J. Cannard, R.J.D. Tilley, New intergrowth phases in the ZnO–In_2O_3 system, J. Solid State Chem. 73 (1988) 418.
[26] N. Kimizuka, M. Isobe, N. Nakamura, Synthesis and single-crystal data of homologous compounds $In_2O_3(ZnO)_m$ ($m=3$, 4 and 5), $InGa_2O_4(ZnO)_3$ and $Ga_2O_3(ZnO)_m$ ($m=7$, 8, 9 and 16) in the In_2O_3–$ZnGa_2O_4$–ZnO system, J. Solid State Chem. 116 (1995) 170.
[27] M.C. McCoy, R.W. Grimes, W.E. Lee, Planar intergrowth structures in the ZnO–In_2O_3 system, Philos. Mag. A 76 (1997) 1187.
[28] V.L. Bulatov, R.W. Grimes, A.H. Harker, Mobility of ions in lanthanum fluoride nanoclusters J. Materials-e. 49(2) (1997).
[29] V.L. Bulatov, R.W. Grimes, A.H. Harker, Low frequency oscillations in nanoclusters of lanthanum trifluoride, Philos. Mag. Lett. 77 (1998) 267.
[30] M. Zacate, R.W. Grimes, P.D. Lee, Simulating the evolution of an atomic layer of neon or argon on a calcium (111) surface using atomistic based cellular automata rules, U.S. Air Force European Office of Aerospace Research and Development (EOARD) Report F6 1 708-96-W0300.